BASIC SCIENCE

Nanomedicine: Nanotechnology, Biology, and Medicine
23 (2020) 102095

Original Article

nanomedjournal.com

Co-delivery of *Poria cocos* extract and doxorubicin as an 'all-in-one' nanocarrier to combat breast cancer multidrug resistance during chemotherapy

Yanan Li, PhD[a,1], Xiaolian Li, MS[a,1], Yang Lu, PhD[b,1], Birendra Chaurasiya, PhD[a], Gujie Mi, PhD[c], Di Shi, PhD[c], Daquan Chen, PhD[d], Thomas J. Webster, PhD[c,*], Jiasheng Tu, PhD[a,**], Yan Shen, PhD[a,**]

[a]*Department of Pharmaceutics, School of Pharmacy, China Pharmaceutical University, Nanjing, China*
[b]*Beijing University of Chinese Medicine, Beijing, China*
[c]*Department of Chemical Engineering, 313 Snell Engineering Center, Northeastern University, Boston, USA*
[d]*School of Pharmacy, Yantai University, Yantai, China*

Revised 26 July 2019

Abstract

Recent studies have indicated that multidrug resistance (MDR) can significantly limit the effects of conventional chemotherapy. In this study, PT (Pachymic acid and dehydrotumulosic acid) are the two major triterpenoid components purified and identified in *P. cocos*. A liposomal co-delivery system encapsulating doxorubicin (DOX) and PT was prepared. Notably, the mechanism of PT reversed P-glycoprotein (P-gp) mediated MDR mainly relied on the inhibition of the P-gp function, which further decreased the levels of P-gp and caveolin-1 proteins. In drug-resistant MCF cells, co-administration with 5 μg/ml PT significantly enhanced sensitivity of DOX. Finally, liposome-mediated co-delivery with PT significantly improved the anti-tumor effect of DOX in tumor-bearing mice when compared to other single therapy groups. In conclusion, this study showed for the first time that DOX and PT act synergistically as an "all-in-one" treatment to reverse MDR during tumor treatment and, thus, should be studied further for a wide range of anti-cancer applications.

Key words: Triterpenoids; DOX; Reverse multidrug resistance; Antitumor; Cancer; Nanomedicine

Conventional chemotherapy, which often involves toxic drugs (such as DNA alkylating agents), is a primary treatment option for various cancers.[1] However, these regimens can induce multidrug resistance (MDR), which significantly limits the outcomes of chemotherapy.[2] MDR can develop over multiple rounds of continual chemotherapy and *via* various molecular mechanisms, including the regulation and deregulation of drug influx,[3] mutation of drug targets, activation of DNA repair mechanisms and deregulation of apoptosis.[4] Therefore, achieving an amplified anti-tumor effect first requires an understanding of the MDR pathway, followed by the identification of highly efficient and minimally toxic agents with MDR reversing properties that can be combined with chemotherapeutic agents[5]; it is only when these conditions are satisfied that we will have true anti-cancer approaches.

Recently, scientists have explored promising combination therapeutic approaches intended to overcome MDR against cancer chemotherapeutic agents *via* synergistic/additive effects. In contrast to mono-chemotherapies, a combination therapy could sensitize the tumor to drugs, modulate different cancer cell signaling pathways and enable the delivery of lower doses of each drug, which could improve clinical outcomes while reducing adverse effects. Accordingly, many groups have focused on combination therapies involving chemotherapeutic drugs and MDR reversing agents.[6]

To date, many synthetic[7–9] and natural MDR reversing agents have been identified.[10,11] Still, these effective agents have many clinical drawbacks, including a single mechanism of action, poor selectivity and a narrow therapeutic index. Accordingly, the selection of appropriate MDR reversing agents with low levels of

Conflict of interest: The authors declare no conflict of interests.

*Correspondence to: T. J. Webster, Department of Chemical Engineering, 313 Snell Engineering Center, Northeastern University, Boston, USA.

**Corresponding authors at: State Key Laboratory of Natural Medicines, Department of Pharmaceutics, China Pharmaceutical University, Nanjing, China.

E-mail addresses: th.webster@neu.edu, (T.J. Webster), jiashengtu@cpu.edu.cn, (J. Tu), shenyan19820801@126.com. (Y. Shen).

[1] These authors contributed equally to this work.

https://doi.org/10.1016/j.nano.2019.102095
1549-9634/

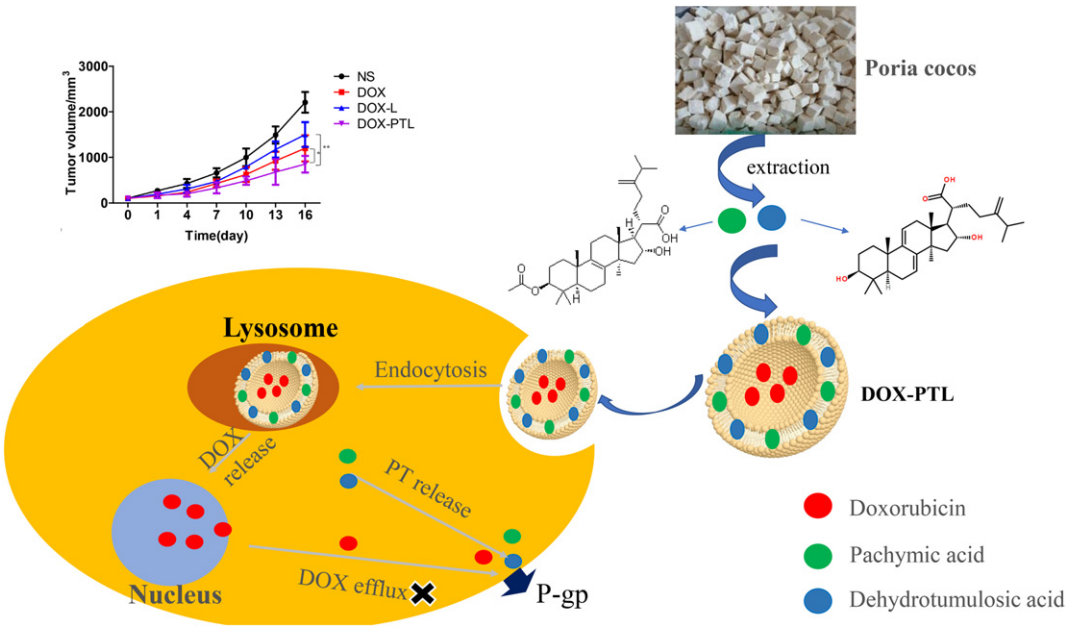

Figure 1. The pachymic acid and dehydrotumulosic acid extracted from *Poria cocos* could be used as a reversal drug resistance agent and are co-loaded with DOX in liposomes to reverse the resistance of tumor cells to chemotherapeutic drugs, achieving enhanced sensitized chemotherapy.

toxicity and high levels of efficiency has elicited considerable interest in the field of cancer chemotherapy. Recently, scientists have explored the field of traditional Chinese medicine (TCM) as a source of alternative treatments for cancer, given the relative safety and multi-mechanistic actions of TCM components.

The field of TCM is replete with natural components which target disease through multiple channels. Plenty of studies have demonstrated that triterpenoids can efficiently inhibit the activity in many MDR cell lines with different mechanisms, including interactions with the P-gp active site, stimulating the activity of the P-gp ATPase or inhibiting the photoaffinity of drugs.[12] Cheng et al. reported that tannic acid, a TCM triterpenoid component, helped to promote apoptosis in gemcitabine-resistant PANC-1 and MIA Paca-2 pancreatic cancer cell lines.[13] Mechanistically, tannic acid activates the heat-shock response, as well as genes involved in the endoplasmic reticulum protein reaction, to induce stress. This process also enhances the expression of XBP-1s, ATF4, Hsp70, CHOP and phospho-eIF2α, which further promote apoptosis. Kim et al found that an extract of *Poria* spp. could reduce the efflux of digoxin and daunorubicin in cells with high MDR1 expression.[14] These experiments suggest that triterpenoids exhibit certain anti-tumor effects and may partially reverse MDR in tumor cells by inhibiting the activity of P-gp. *Poria cocos* has many functions, such as anti-inflammatory and anti-tumor effects. Researchers have also found that the ethanol extracts of *Poria cocos* possess reverse-MDR ability, so *Poria cocos* was chosen as a Chinese herb here which is rich in triterpenoids. Accordingly, chemotherapeutic drugs could potentially be combined with triterpenoids with multifunctional MDR reversing activities.

Doxorubicin (DOX) is considered a classical chemotherapy drug and is frequently used to treat multiple myeloma and many solid tumors, including breast, lung, gastric, ovarian and thyroid cancers. Beyond the emergence of MDR, however, the clinical use of DOX is severely limited by the risk of progressive, dose-dependent cardiomyopathy and irreversible congestive heart failure.[15,16] Therefore, efforts in the field of DOX research are currently focused on maintaining drug efficacy while reducing toxicity.

In this study, we attempted to construct an 'all-in-one' system that would deliver DOX and a triterpenoid extract of pachymic acid and dehydrotumulosic acid (PT) in a liposomal carrier (DOX-PTL). A mixture of triterpenoids was extracted from *Poria cocos* as a multifunctional MDR reverse agent which contains pachymic acid and dehydrotumulosic acid. In addition, PT as a multi-component MDR reverser has higher safety than conventional chemotherapeutic drugs, and sensitized DOX to kill tumor cells specifically in drug-resistant tumors. Moreover, the liposome nanosystem would further increase the enhanced permeability and retention (EPR) effect at the tumor site which enhances targeting to tumors for DOX and PT, avoiding toxicity to normal tissue. Finally, the liposomes, loaded with DOX and PT simultaneously, can prevent severe toxic side-effects caused by *in vivo* pharmacokinetic differences between PT and DOX. In our study, first, triterpenoids were extracted from *Poria cocos*, and the main PT components were identified and characterized. Next, the possible mechanism by which PT reverses MDR in tumor cells was investigated. Subsequently, both PT and DOX were loaded into liposomes to construct an all-in-one nanoparticle delivery system, and the release of PT and DOX release from the liposomes was studied. Additionally, *in vitro* cytotoxicity, cellular uptake and *in vivo* tumor targeting studies were conducted to evaluate the synergistic effects of PT and DOX (Figure 1).

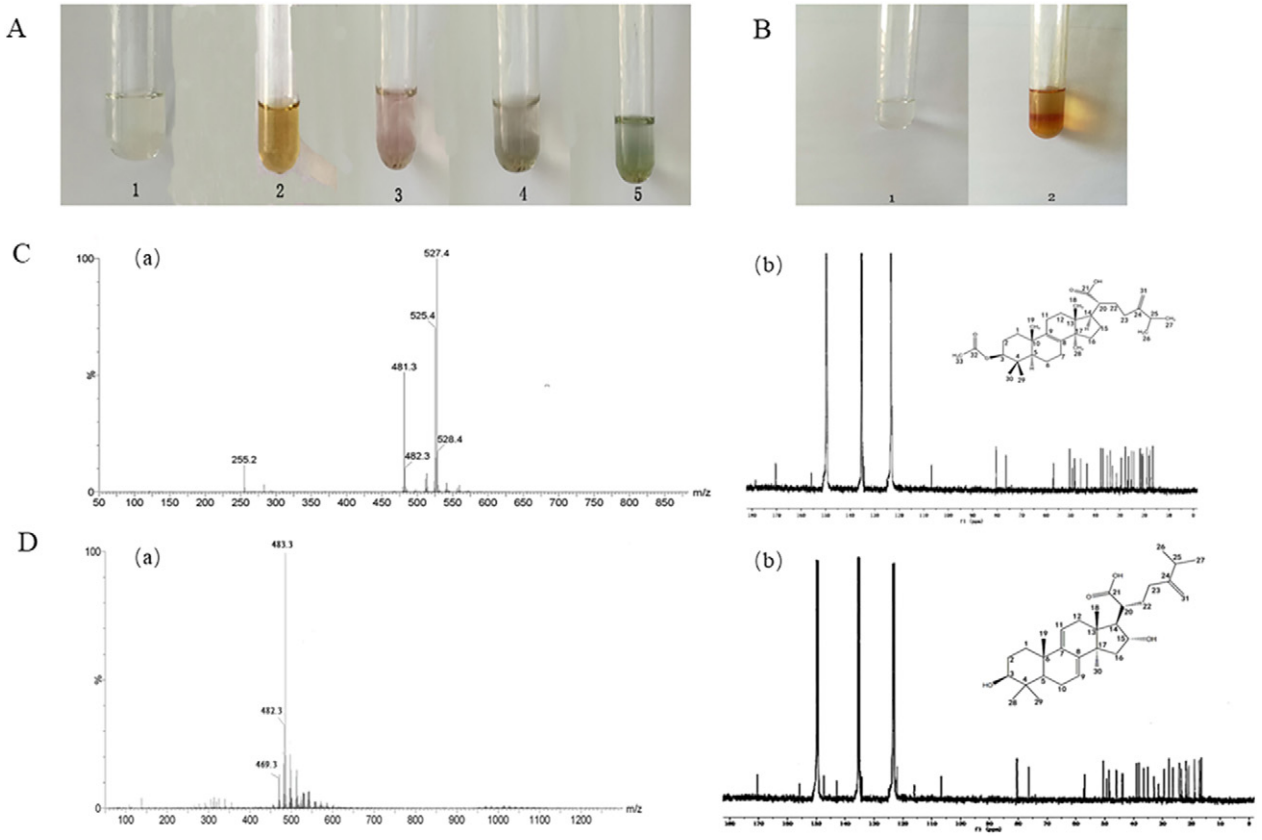

Figure 2. Color changes associated with (**A**) the Liebermann–Burchard reaction and (**B**) the Salkowski reaction. MS (**C**) and ^{13}C-NMR spectra (**D**) of pachymic acid. EMS (**a**) and ^{13}C-NMR spectra (**b**) of dehydrotumulosic acid.

Taken together, the analyses proved that the combined administration of a synthetic chemotherapeutic agent and a natural drug more effectively treated a solid tumor and induced a lower level of systemic toxicity, compared to mono-therapy.

Methods

Materials

Lecithin and cholesterol were purchased from Avanti Polar Lipids, Inc. (Alabaster, AL, USA). Doxorubicin (DOX) was purchased from Huafeng United Technology (Beijing, China). MTT ((3-(4,5-dimethyl-thiazol-2-yl)-2,5-diphenyl-tetrazolium bromide) was obtained from the Shanghai Institute of Cell Research (Shanghai, China). 1,1′-Dioctadecyl-3,3,3′,3′-tetramethyl indotricarbocyanine iodide (DiR) was obtained from Sigma Chemical Co., Ltd. (St. Louis, MO, USA). All reagents were of analytical grade and used without further purification.

Methods

In vivo evaluation

Development of a tumor model. Female BALB/c nude mice (body weight: 20 ± 2 g, age: 3-4 weeks) were purchased from Qinglongshan Farms (Nanjing, China) and acclimated according to the standard guidelines set by China Pharmaceutical University for the handling of experimental animals. To develop tumor model animals, approximately 1×10^6 MCF/ADR cells were injected subcutaneously into the right forelimb armpit of each mouse. Tumor growth was monitored. The tumor volume was calculated using the formula $V = AB^2/2$, where A and B are the maximum and minimum diameters of the tumor, respectively.

In vivo distribution. To evaluate *in vivo* distribution, DiR-loaded liposomes (DiR-Lip) were prepared using the thin film method. Once the tumor sizes reached 150 mm^3, the tumor-bearing mice were randomly divided into two groups (n = 6 each) and were treated intravenously (IV) with free DiR or DiR-Lip adjusted to yield equivalent doses of 2 mg/kg DiR. The distribution of DiR was confirmed by imaging the treated mice using an IVIS device at time points of 2, 4, 6, 12 and 24 h.

Anti-tumor efficacy. Once the tumor size reached 100-150 mm^3, the mice were randomly divided into four groups (n = 7 each): saline, DOX solution, DOX-L and DOX-PTL. In each formulation, the DOX concentration was adjusted to a dose of 2.5 mg/kg. Next, five 200-μL volumes of each formulation were injected by IV into the respective mice *via*

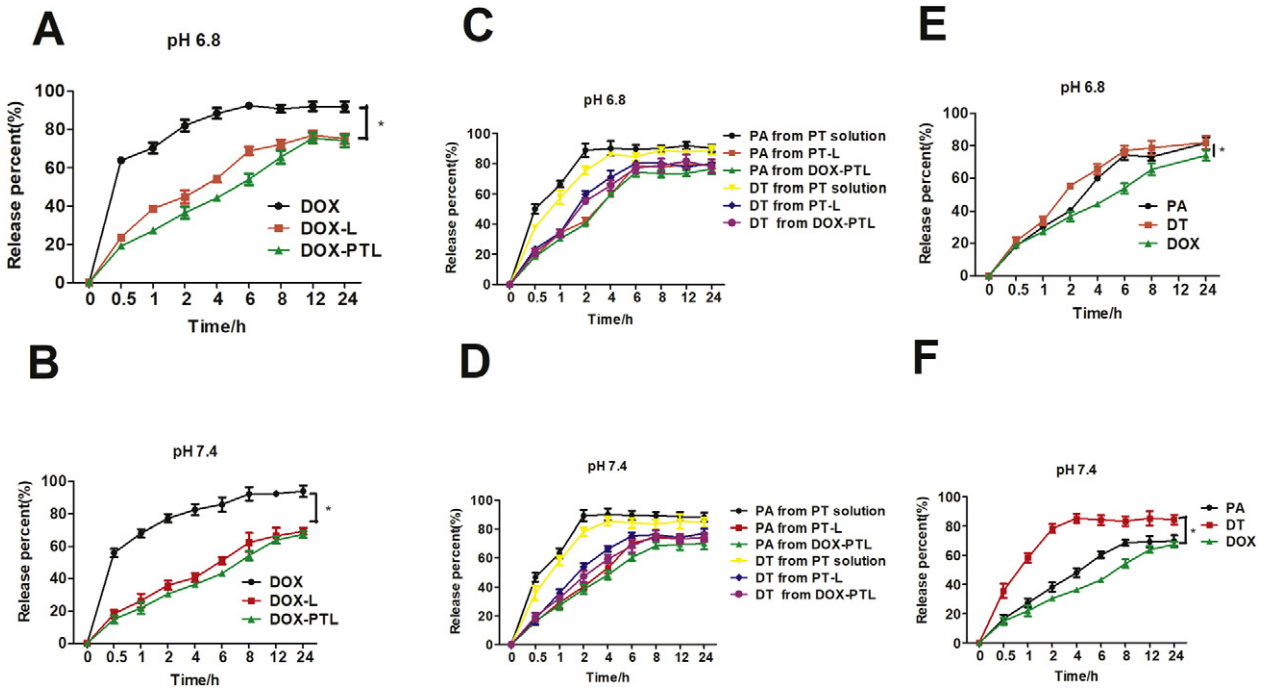

Figure 3. The release behavior of DOX from a DOX solution, DOX-L and DOX-PTL (n = 4 each) at pH levels of 6.8 (**A**) and 7.4 (**B**). Release behaviors of pachymic acid (PA) and dehydrotumulosic (DT) from a PT solution, PT-L and DOX-PTL (n = 3 each) at pH levels of 6.8 (**C**) and 7.4 (**D**). Release behaviors of pachymic acid (PA), dehydrotumulosic acid (DT) and DOX from DOX-PTL at pH levels of 6.8 (**E**) and 7.4 (**F**). Data are presented as mean ± SD (n = 3). *$P < 0.05$.

the tail vein at 3-day intervals. Changes in the tumor size and body weight were measured at 2-day intervals. Finally, histopathological images were evaluated for the organs, containing the liver, lung, spleen, kidney, and heart obtained from tumor-bearing mice.

Data analysis

All analyzed data are presented as the mean ± standard deviation (SD). ANOVA followed by Student's t tests (SPSS 17.0, China) was used to analyze the results. Accordingly, *$P < 0.05$ indicated statistical significance and **$P < 0.01$ as well as ***$P < 0.001$ were highly significant compared to the indicated groups.

Results

PT extraction and identification

Lyophilization of the PT extract yielded a yellow powder at a very low yield (0.45%). Three reaction tests were used to identify the extracts. First, during the Liebermann–Burchard reaction, the test sample (no. 1) was initially colorless (Figure 2, *A*). After the addition of concentrated sulfuric acid, the sample changed to an orange-brick red color (no. 2) and subsequently to reddish-violet, bluish-green and green colors (no. 3, 4, and 5, respectively). This pattern of color changes confirmed the presence of triterpenoids. The Rosen–Heimer reaction was conducted next, and the change of the silica gel plate color to purple confirmed the presence of triterpenoids. Finally, a Salkowski reaction was conducted. As shown in Figure 2, *B*, the sample (no. 1) changed to an orange-red color at the bottom (no. 2) due to the stratification of terpenoids in the presence of concentrated sulfuric acid, and the upper layer changed to a florescent green color. Again, this pattern confirmed the presence of terpenoids in the extract.

Further, triterpenoids present in the extract, specifically PT, were purified and identified using MS and ^{13}C NMR, and the results are shown in Figure 2, *C-F*. In Figure 2, *C*, the MS spectrum includes a characteristic peak at 528 m/z, which was further confirmed by ^{13}C NMR. The peaks at 178.6 (C-21) and 170.4 (MeCO) were assigned to carboxyl groups, while the peaks at 80.4 (C-3) and 76.4 (C-16) correspond to two oxymethine resonances of pachymic acid (Figure 2, *D*). This chemical shift in the ^{13}C NMR spectrum indicated the presence of pachymic acid, consistent with previously reported results.[17,18] Similarly, Figure 2, *E* depicts the characteristic MS peak at 484 m/z and ^{13}CNMR chemical shifts (Figure 2, *F*) consistent with dehydrotumulosic acid, as described in previous reports.[19] Moreover, the resonance peak at 76.4 (C-16), which corresponds to oxymethine, confirmed the presence of dehydrotumulosic acid. The ^{13}C NMR signal at 80.4 (C-3) was attributed to an oxygen-bearing methine. In addition, the ^{13}C NMR signal at 16.5 (C-29) caused by Me-29 also confirmed the existence of a -CH_3 group. The contents of these triterpenoids in the extract were further quantified using a UV spectrophotometer. A total yield of 83.52 ± 0.79% was calculated.

Characterization of DOX-PTL

The surface morphology of DOX-PTL was characterized using TEM. A representative image is shown in Figure S1, *A*. Notably, DOX-PTL exhibited a layered morphology with relatively uniform particle diameters of 100-200 nm.

Figures S1, *B* and S1, *C* respectively depict the particle size distribution and zeta potential of DOX-PTL. The particles had a uniform size of 158.5 ± 1.1 nm and PTI of 0.251 ± 0.010, with a measured zeta potential of 34.22 ± 5.85 mV. The calculated % EE values of doxorubicin, tannic acid and dehydrotumulosic acid were 93.50 ± 1.43%, 73.20 ± 1.57% and 82.97 ± 2.23%, respectively.

Release behavior of liposomes

An *in vitro* release experiment was conducted at pH levels of 6.8 and 7.4 to stimulate the *in vivo* release of the loaded content from liposomes in normal and tumor tissues, respectively. As shown in Figure 3, no differences in release behavior were observed at different pH levels. Figure 3, *A* and *B* demonstrated that within a 24-h period, the cumulative release of DOX from the DOX solution was comparatively more rapid (~90%) than the release from DOX-L and DOX-PTL (~60%). The slightly slower release of DOX from DOX-PTL relative to DOX-L may be due to the hydrophobic nature of the drug (extract) loaded between the phospholipid layers of the liposome. Specifically, the liposomal matrix may delay the release of DOX from the liposome. The release patterns of tannic acid (PA) and dehydrotumulosic acid (DT) are shown in Figure 3, *C* and *D*. PA and DT were released very rapidly (within 2-4 h) and completely formed a PT solution. By contrast, the release rates of these triterpenoids from DOX-PTL were > 70% within 6-8 h, while DOX was released completely after 12 h. The release behaviors of DOX, PA and DT from DOX-PTL are shown in Figure 3, *E* and *F*. Here, the release rates of PA and DT were higher than that of DOX.

Stability of DOX-PTL

To assess stability, DOX-PTL samples were stored for 1 month at room temperature or 4 °C. The results are shown in Figure S2. The liposomes stored at room temperature formed aggregates during the 30-day period, and some leakage of DOX, tannic acid and dehydrotumulosic acid was detected. However, the liposomes stored at 4 °C exhibited no changes in appearance or particle size (Table 1), and no obvious leakage of DOX, tannic acid or dehydrotumulosic acid. This finding indicated that 4 °C is a suitable storage condition for DOX-PTL.

Cytotoxicity of PT and its effect on MDR reversal

As shown in Figure 4, *A-C*, the triterpenoid extract had an inhibitory effect on A549 cells and induced greater cytotoxicity at 48 h relative to 24 h. The viabilities of cells exposed to 400 μg/ml triterpenoids were 61.02% at 24 h and only 25.10% at 48 h, indicating a directly proportional relationship between cell viability and time. However, in HepG-2 cells, triterpenoid induced obvious cytotoxicity at a concentration of only 20 μg/ml, and the cell survival rate decreased below 80% at 200 μg/ml. By contrast, MCF-7 cells were less susceptible to PT-mediated toxicity, with an IC_{50} above 400 μg/mL. In summary, the triterpenoid extract induced direct inhibitory effects on different tumor cell lines, and the strongest effect was observed in HepG-2 cells.

Table 1
Stability investigation of DOX-PTL (n = 3, mean ± SD).

	Day 0	Day 30, room temperature	Day 30, 4 °C
Diameter (nm)	163.5 ± 2.8	208.1 ± 3.5	167.3 ± 2.3
PDI	0.230 ± 0.018	0.225 ± 0.023	0.251 ± 0.021
EE (%) (DOX)	91.56 ± 1.32	82.30 ± 2.53*	90.38 ± 1.09
EE (%) (paychmic acid)	71.36 ± 1.28	43.25 ± 1.23*	70.25 ± 2.38
EE (%) (dehydrotumulosic acid)	81.35 ± 2.09	58.21 ± 1.89*	79.95 ± 1.76

When compared to day 0, *$P < 0.05$.

Next, the cytotoxicity of DOX was measured in MCF and MCF/ADR DOX-resistant cells. As shown in Figure 4, *C* and *D*, IC_{50} results of 0.467 ± 0.013 and 18.237 ± 0.238 μg/ml were obtained for MCF and MCF/ADR DOX-resistant cells, respectively. Accordingly, a DOX resistance factor (RF) of 38.832 ± 1.1456-fold was calculated, indicating that MCF/ADR cells were highly resistant to this drug. Additionally, IC_{50} values of 6.701 ± 0.174 and 17.956 ± 1.101 μg/ml were calculated for A549 and A549/CDDP cells, yielding a drug RF of 2.678-fold. As the RF for A549/CDDP cells was relatively lower than that obtained with MCF/ADR cells, the latter were chosen for further study.

Then, the effect of PT to reverse MDR was conducted. As shown in Figure S3, *A*, PT had a slightly toxic effect on MCF/ADR cells, with survival rates >90% after 48 and 72 h of exposure to 50 μg/ml. Accordingly, PT concentrations of 5, 25 and 50 μg/ml were selected for subsequent experiments to evaluate the reverse-resistance effect (Figure S3, *A*). As shown in Figure S3, *B*, VP exhibited a similarly low level of cytotoxicity in MCF/ADR cells, and an experimental concentration of 25 μg/ml was selected.

Moreover, a 50 μg/ml concentration of PT had a slight effect on A549/CDDP cells (Figure S3, *C*). The survival rate of 85% suggests that these agents could be used as sensitizers. Moreover, exposure to 25 μg/ml VP yielded a cell viability rate of 80% (Figure S3, *D*). Accordingly, the selected maximum concentrations of PT and VP were 50 and 25 μg/ml, respectively. For subsequent MDR reversal studies, the triterpenoid concentrations were set at 5, 25 and 50 μg/ml, and the VP concentration was set at 25 μg/ml.

Figure 5, *A*, *B* and Table 2 demonstrate the effect of triterpenoids on MDR reversal in MCF/ADR cells. As shown in

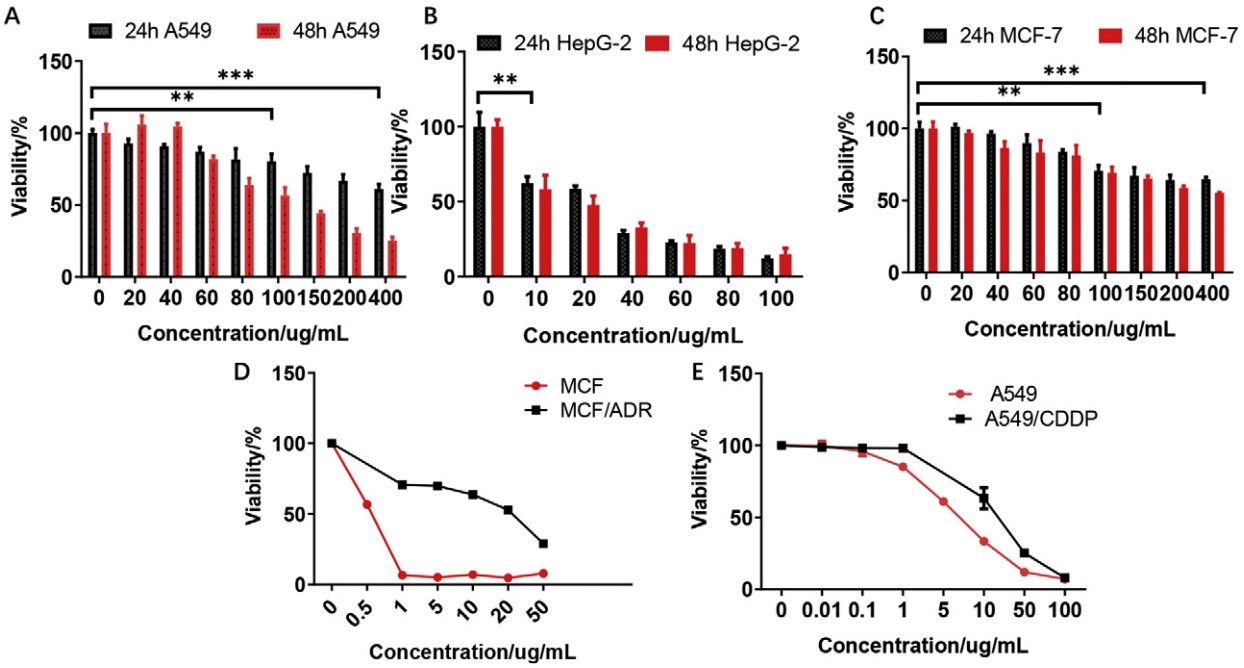

Figure 4. Cell viability of A549 (**A**), HepG-2 (**B**) and MCF-7 cells (**C**) treated with PT (n = 4). Cytotoxicity of DOX on MCF and MCF/ADR cells (**D**) and of CDDP in A549 and A549/CDDP cells (**E**). Data are presented as mean ± SD (n = 4). $^{**}P < 0.01$, $^{***}P < 0.001$, *vs* the viability at the concentration of 0.

Table 2, the addition of 5 μg/ml PT reduced the IC_{50} of DOX 18.237 ± 0.258 to 10.967 ± 0.042 μg/ml, yielding a reverse-RF of 1.66-fold. Moreover, the reverse-RFs in cells treated with DOX plus triterpenoids at 25 and 50 were 13.92- and 39.99-fold higher than that achieved with DOX alone, and these differences were significant. The reverse-RF in the positive control group (VP) was 37.60-fold, indicating that the ability of triterpenoids to reverse MDR is concentration-dependent. Additionally, the RF increased significantly at 72 h relative to 48 h, indicating a time-dependency of this reversal ability. At 48 h, the CI was >1 at 5 μg/ml triterpenoids and 20 μg/ml DOX but <0.9 for all other DOX concentrations. However, at a PT concentration of 25 or 50 μg/ml, the CIs at all DOX concentrations were < 0.4, indicating a significant synergistic effect of 25 or 50 μg/ml PT and DOX. At 72 h, the CIs were > 0.9 at a PT concentration of 5 μg/ml and DOX concentrations of 10, 20 and 50 μg/ml but <0.9 at all other DOX concentrations. At PT concentrations of 25 and 50 μg/ml, the CIs were < 0.9 only at DOX concentrations of <50 μg/ml.

Figure 5, *C*, *D* and Table 3 present the CDDP-resistance reversing effects of PT in A549/CDDP cells. The addition of PT decreased the IC_{50} values of CDDP in A549/CDDP cells, compared to CDDP alone. At a PT concentration of 5 μg/ml, the CIs were > 0.9 at CDDP concentrations of 1-10 μg/ml but <0.9 at all other concentrations. At a PT concentration of 25 μg/ml, the COs were < 0.9 at CDDP concentrations >5 μg/ml, suggesting a synergistic enhancement of the anti-tumor effect of CDDP. At a PT concentration of 50 μg/ml, all CIs were < 0.4, indicating a strengthening of the synergy between CDDP and PT.

Mechanism by which PT reverses MDR

Effect of PT on P-gp function

P-gp function was investigated by detecting the transfection of Rh123, a substrate of P-gp. Under conditions of relatively high P-gp activity, strong drug efflux reduces the intracellular accumulation of Rh123. As shown in Figure 6, *A*, no significant differences in fluorescence intensity were observed in cells treated with 5 or 25 μg/ml PT, compared to untreated negative control cells. By contrast, significantly enhanced fluorescence was observed in cells treated with 50 μg/ml triterpenoids. The lack of a significant difference in fluorescence intensity between the positive VP group and 50 μg/ml PT group indicates the significant inhibitory effect of this concentration of PT on P-gp function.

Effect of PT on P-gp expression

P-gp can attenuate the effects of chemotherapeutic drugs by enhancing the drug efflux effect. P-gp is overexpressed in almost all types of cancer. As this high expression correlates with drug resistance in tumor cells, the inhibition of P-gp expression or function has become a primary target of attempts to enhance drug sensitivity. In this study, western blotting was used to detect changes in P-gp expression in MCF/ADR and MCF cells (Figure 6, *B*). Notably, higher P-gp levels were observed in MCF/ADR cells than in MCF cells. A quantitative analysis revealed that the P-gp content in MCF/ADR cells was 7.27-fold higher than that in MCF cells (Figure 6, *C*). The change in P-gp levels after triterpenoid treatment was also evaluated. Although the P-gp level remained largely stable in cells treated with 5 μg/ml triterpenoids, exposure to 25 or 50 μg/ml triterpenoids

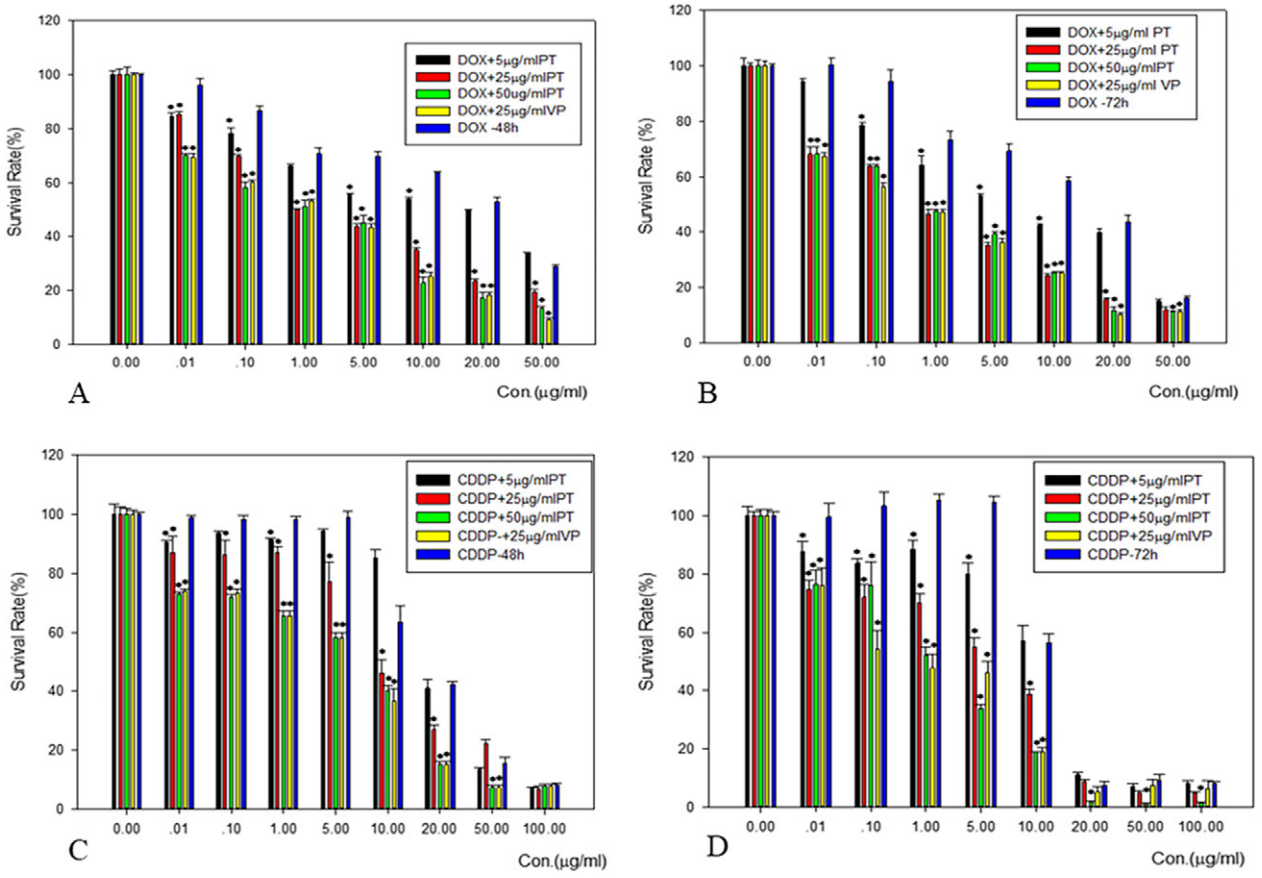

Figure 5. (**A, B**) Cytotoxicity of DOX when combined with PT/VP on MCF/ADR cells ($n = 4$) (*$P < 0.05$ *vs.* DOX alone). (**C, D**) Cytotoxicity of CDDP when combined with PT/VP on A549/CDDP cells. Data are presented as mean ± SD ($n = 4$) (*$P < 0.05$, *vs.* DOX alone).

respectively led to moderate and significant decreases in the P-gp levels. This finding indicates that PT could inhibit the expression of P-gp, consistent with the findings from Rh123 transfection experiments. Moreover, the ability of PT to inhibit the expression of P-gp appeared to be concentration-dependent.

Effect of lipid raft stability

Caveolin-1 is a small (molecular weight: 21-24 kDa) transmembrane protein which is co-expressed with P-gp in lipid rafts. Changes in caveolin-1 levels affect the stability of lipid rafts, leading to MDR. Accordingly, caveolin-1 is often used as an indicator of lipid raft stability. Here, the localization and aggregation of caveolin-1 were investigated in cells treated with different concentrations of PT, as shown in Figure 6, *D*. In untreated cells and those exposed to 5 μg/ml PT, caveolin-1 aggregated on the cell membranes. However, treatment with 25 or 50 μg/ml PT led to the relative scattering of caveolin-1, indicating that the stability of lipid rafts had been affected. Simultaneously, the fluorescence intensity gradually decreased, indicating that the caveolin-1 protein level decreased as the concentration of PT increased.

To further verify the above results, western blotting was used to detect the levels of caveolin-1. As shown in Figure 6, *E*, caveolin-1 was expressed onboth MCF and MCF/ADR cells, and the level in the latter was 7.38-fold higher than that in the former. In other words, MCF/ADR cells strongly expressed caveolin-1, consistent with other studies.[20] Moreover, treatment with 5 μg/ml PT had almost no effect on the caveolin-1 levels in MCF/ADR cells, whereas treatment with 25 or 50 μg/ml PT significantly reduced caveolin-1 levels (Figure 6, *F*). In other words, exposure to high concentrations of PT inhibited the expression of caveolin-1.

Effect of PT on the physical fluidity of the cell membrane

In the cell membrane, changes in physical fluidity may induce changes in various functional aspects, such as permeability and the functions and activities of some proteins. Accordingly, altered physical fluidity may affect the function of P-gp. To verify whether PT induced changes in cell membrane fluidity, the fluorescence polarization (P), anisotropy (γ) and membrane microviscosity (η) were measured in cells labeled with DPH, a dye used to determine cell membrane fluidity. Here, larger P, γ and η values indicate a reduction in cell membrane fluidity. As shown in Table 4, no significant

Table 2
The reversal effect of PT and VP on MCF/ADR cells.

	IC50 (μg/ml)		MR	
	48 h	72 h	48 h	72 h
DOX	18.237 ± 0.258	14.885 ± 1.524	-	-
DOX + 5 μg/ml PT	10.967 ± 0.042*	4.208 ± 0.444**	1.66	3.537
DOX + 25 μg/ml PT	1.310 ± 0.106**	0.935 ± 0.254**	13.92	15.92
DOX + 50 μg/ml PT	0.456 ± 0.107**	0.266 ± 0.066**	39.99	55.96
DOX + 25 μg/ml VP	0.485 ± 0.098**	0.253 ± 0.036**	37.60	58.83

Data are presented as mean ± SD (n = 4). (*P < 0.05, **P < 0.01 *vs.* DOX alone).

Table 3
The reversal effect of PT and VP on A549/CDDP cells.

	IC50(μg/ml)		MR	
	48 h	72 h	48 h	72 h
CDDP	17.956 ± 1.101	8.495 ± 0.700	-	-
CDDP+5 μg/ml PT	17.833 ± 0.921	6.176 ± 0.716	1.007	1.370
CDDP+25 μg/ml PT	7.784 ± 0.342*	1.373 ± 0.317**	2.307	6.187
CDDP+50 μg/ml PT	1.537 ± 0.450**	0.491 ± 0.015**	11.682	17.301
CDDP+25 μg/ml VP	1.507 ± 0.380**	0.324 ± 0.010**	11.915	26.219

Data are presented as mean ± SD (n = 4). (*P < 0.05, **P < 0.01 *vs.* CDDP alone).

changes in these values were observed in the cells after treatment, thus, indicating no significant effect on cell membrane fluidity.

DOX-PTL cytotoxicity study

The MTT analysis was used to assess the cytotoxicity of blank liposomes. Here, the cell viability was >90% after a 48-h incubation, indicating that the blank liposomes were not toxic. As shown in the Figure 7, *A*, DOX-PTL was associated with the strongest cytotoxic effect, which verified the synergistic effects of the components. The triterpenoids were thought to reverse MDR and, thus, increase sensitivity to DOX. Moreover, the lack of a significant difference in cytotoxicity between the DOX-L and free DOX groups indicated that DOX was almost completely released from the liposomes. A comparison of DOX-PTL with DOX-L at DOX concentrations of 1, 5, 10 and 20 μg/ml yielded CI values of <0.4, further confirming the synergistic effects of DOX and PT in the liposomes.

P-gp and caveolin-1 levels in response to DOX-PTL

The levels of P-gp and caveolin-1 were determined in cells treated with DOX-PTL and DOX solution (Figure 7, *B*, *C*). The P-gp level decreased significantly after treatment with DOX-PTL but not with DOX. This result suggests that the former could reverse MDR, consistent with the results of the cytotoxicity assay. In addition, the caveolin-1 content remained almost unchanged after treatment with DOX-PTL, whereas treatment with free DOX enhanced the expression of this lipid raft marker. In other words, DOX alone could easily induce drug resistance, whereas the all-in-one DOX-PTL could reverse this trend according to the above-described mechanisms.

Uptake of fluorescence/DOX-liposomes (DOX-FL)

The cellular uptake of liposomes and free DOX is shown in Figure 7, *D*. Here, the fluorescence intensity in the free DOX group increased as the incubation time increased from 2 to 6 h, and peaked at the latter time point. In the DOX-L and DOX-FL group, the fluorescence intensities increased gradually up to 4 h and plateaued thereafter, indicating a saturation of liposome uptake. Moreover, the fluorescence intensities of the DOX-L and DOX-FL group were nearly identical at each time point, indicating no significant difference in the cellular uptake of the two liposomal preparations. Potentially, these formulations exhibited a similar size and surface zeta potential, which are key factors affecting liposomal uptake.

In vivo study

IVIS fluorescence imaging was used to detect the accumulation of liposomes within the tumors of MCF/ADR tumor-bearing mice. Figure 8, *A* presents real-time images of DiR and DiR-Lip accumulation at 2, 4, 6, 12 and 24 h post-administration. DiR fluorescence was distributed almost completely throughout the liver within 12 h, whereas preferential accumulation corresponding to the liposomes could be detected in the tumors after 4 h. Moreover, DiR-Lip was most strongly accumulated in the tumor at 12 h, after which time the fluorescence decreased. However, significant DiR intensity was detectable in the tumor at 24 h (Figure 8, *A* and *B*). The tumor-targeting abilities of the liposomes were attributed to the EPR effect. This evidence confirms the potential usefulness of liposomes for the delivery of DOX and PT.

In a study of anti-tumor efficacy, all DOX-treated groups exhibited decreases in tumor size relative to the negative saline-treated group. Notably, DOX-L had a similar inhibitory effect when compared to the free DOX solution. This may be attributed to the incomplete release of DOX from the liposomes when accumulated in the tumor area, as confirmed in Figure 8, *C*. DOX-PTL exhibited the strongest anti-tumor ability when compared with the DOX solution (P < 0.05) and DOX-L (P < 0.01). Again, this finding confirmed the excellent synergistic abilities of DOX and PT to reverse MDR and induce tumor cytotoxicity. Moreover, no losses in body weight or other signs of toxicity, such as diarrhea, were observed in liposome-treated mice, suggesting that the liposome formulation is safe in normal tissue and may increase the biocompatibility of DOX (Figure 8, *D*). All of these results demonstrated the excellent ability of PT to reverse MDR and thus restore DOX sensitivity in cancer cells. Moreover, the DOX-PTL decreased the toxicity of free DOX for the mice by histopathological images of the organs, including the liver, lung, spleen, kidney, and heart obtained from tumor-bearing mice which confirmed its safety (Figure S4). Accordingly, this approach demonstrates promise as an effective anti-tumor therapy.

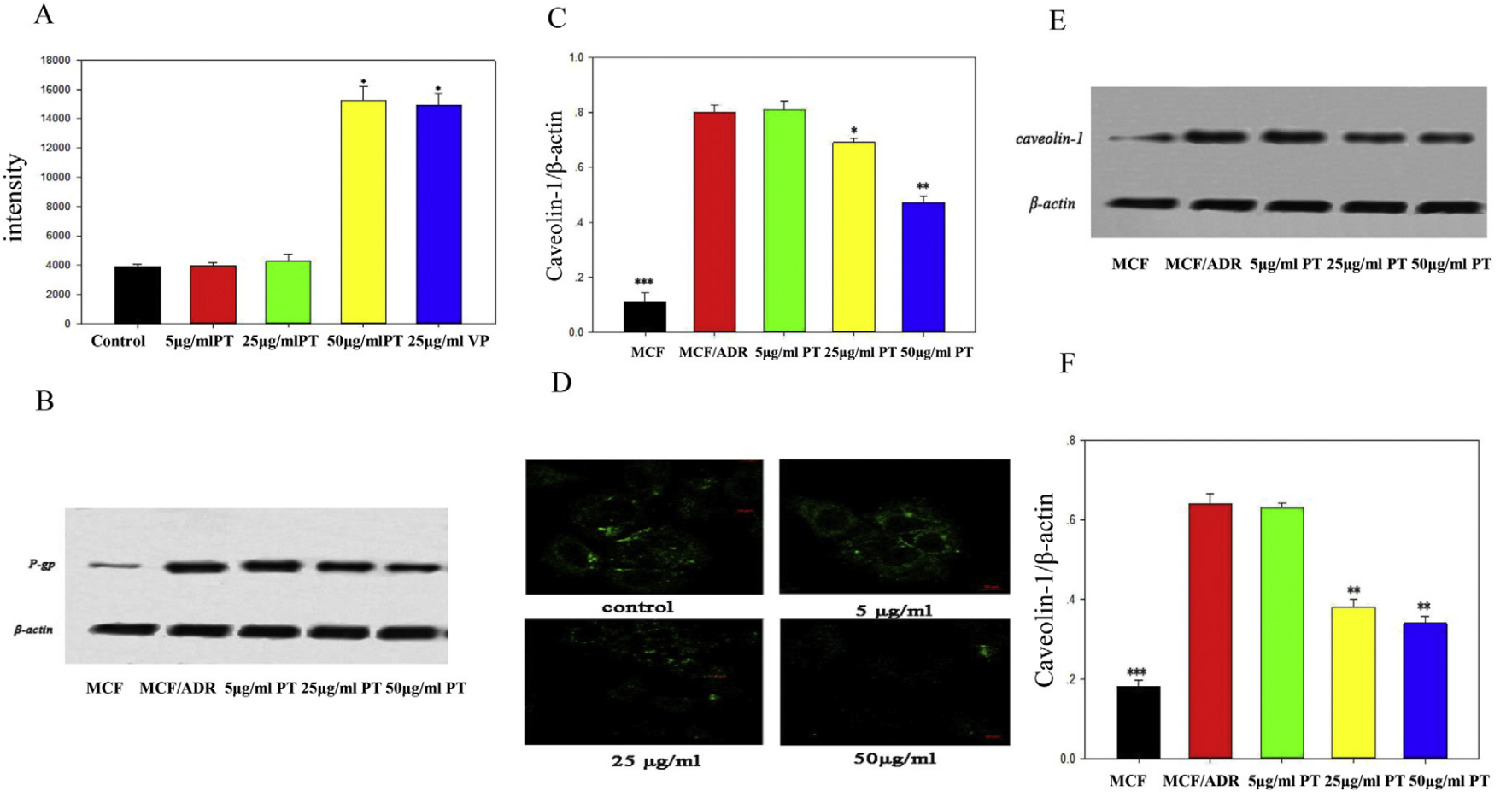

Figure 6. (**A**) The effects of different PT concentrations on intracellular Rh123 accumulation in MCF/ADR cells (n = 3) (*P < 0.05, *vs.* control). P-gp levels in MCF/ADR cells treated with different concentrations of PT (**B**) and the gray analysis (**C**). (**D**) The localization and aggregation of caveolin-1 in cells treated with different concentrations of PT (0, 5, 25 and 50 μg/ml). Expression of caveolin-1 in MCF/ADR cells treated with different concentrations of PT (**E**) and the gray analysis (**F**) (*P < 0.05, ** P < 0.01, *** P < 0.01, *vs.* MCF/ADR group).

Table 4
The change of cell membrane fluidity of MCF/ADR after treatment with different concentrations of PT.

Concentration of PT (μg/ml)	P (mp n = 3)	γ	η
Control	0.2418 ± 0.0027	0.1753 ± 0.0022	2.2173 ± 0.0533
5	0.2396 ± 0.0018	0.1736 ± 0.0014	2.1740 ± 0.0348
25	0.2431 ± 0.0048	0.1764 ± 0.0038	2.2440 ± 0.090
50	0.2486 ± 0.0078	0.1807 ± 0.0062	2.3574 ± 0.1662

Data are presented as mean ± SD (n = 3).

Discussion

In this study, triterpenes were extracted successfully from *P. cocos*, and their ability to reverse P-gp-related MDR in tumor cells both *in vitro* and *in vivo* was studied. In the MTT study on MCF/ADR cells, compared with DOX alone, the cell viability decreased significantly when DOX was administered together with triterpenoids or VP. Moreover, the ability of triterpenoids to reverse MDR is concentration-dependent which was proved on different drug-resistant cells.

Based on the excellent reverse-MDR effect, the in-depth mechanism of PT to reverse MDR was researched. In this study, a comprehensive study of the mechanism of action was revealed for the first time. From the results, it can be found that PT could inhibit P-gp function, and decrease P-gp expression at the same time. This result was consistent with the reference.[21] Besides, this study proved that PT changed the P-gp function as accompanied with changing the stability of the lipid raft instead of the physical fluidity of the cell membrane.

Currently, nano-carriers are commonly constructed for the delivery of single chemotherapeutics. However, the use of a single agent may suffer from severe toxicity at high drug doses and easily develop drug resistance. The co-delivery of multiple chemotherapeutics has been widely studied, such as the combination of gemcitabine and doxorubicin in a hyaluronic acid conjugate[22] and the combination of doxorubicin (DOX) and paclitaxel (PTX) in a polymer–dendrimer hybrid nanoparticle, and can achieve sequential release to inhibit tumors significantly.[23] Moreover, to inhibit MDR and synergistically inhibit tumor growth, co-delivering three chemotherapeutic agents have also been developed such as doxorubicin (DOX), paclitaxel (PTX), and silybin in multilayer nanosystems which showed superior antitumor effects. With an enhanced antitumor effect, multiple chemotherapeutics have also exhibited enhanced toxicity in the reference.[24] Therefore, in our study, pachymic acid and dehydrotumulosic acid as multifunctional MDR reversing agents were first proposed to be co-delivered from liposomes with DOX.

Next, the all-in-one system was constructed to load PT and DOX inside the liposome. The DOX and PT loaded liposomes showed robust stability, efficiently delivering capacity, good biocompatibility and uniform size distribution. Our liposomes revealed high encapsulation efficient along with high drug loading for DOX and PT.

Drug resistance is a major hurdle for efficient chemotherapy. To solve this problem, the combination of chemotherapeutic drugs was introduced for a few options which is accompanied by severe side effects. Our results demonstrated that the combination of PT as a reverse-MDR agent and the chemotherapeutic drug DOX in the liposome had a size of 100 nm which was preferred by tumors due to EPR effects and improved stability in plasma. Moreover, the dose of PT used as a reverse-MDR agent possessed low-toxicity and the "all-in-one" liposome decreased cardiac toxicity of DOX significantly. Furthermore, the release rates of PT were higher than that of DOX at a pH of 6.8 which indicated that in a tumor, PT first released and occupied P-gp to reduce the effect of P-gp on DOX and thereby sensitized the tumor cells to the drug. In the initial set of experiments, PT was shown to be highly compatible with DOX when delivered as a combinational therapy in a liposomal carrier. Accordingly, DOX and PT were encapsulated in liposomes to yield an all-in-one system. Moreover, DOX-PTL exhibited greater antitumor ability when compared with DOX alone. The *in vivo* results also confirmed the excellent synergistic effects of DOX and PT. Compared with the recent combination reports on multiple chemotherapeutics, the selected PT dose in our study showed no obvious toxicity, so that our "all-in-one" design with PT and DOX in liposomes increased safety by increasing the sensitivity of DOX. There have also been some other natural medicines extracted to reverse MDR (such as the quercetin as the P-gp inhibitor) which exhibited excellent antitumor effects when combined with DOX.[25] However, in our study, compared with the reference,[25] marginal benefits with PT/DOX-L compared to using DOX alone were found in the antitumor study. This phenomenon may attribute to the following reasons. First, the ratio of PT to DOX in liposomes may affect the efficacy of the co-loaded liposomes. *In vitro* cytotoxicity results demonstrated that by optimizing drug ratios, the co-delivery of liposomes could result in better antitumor efficacy. In the future, liposomes with different DOX/PT ratios (based on the same dose of DOX) can be prepared to optimize their efficacy in animals. Moreover, the technology of purifying PT needs to be explored to improve its purity to higher than 95%, which would be beneficial to improve its efficacy as an MDR reversal agent. The results warrant further careful consideration of co-delivery strategies for cancer treatment. Furthermore, the mechanism by which PT acts to reverse MDR should be investigated in detail, particularly in the context of liposomal nanocarrier delivery.

Appendix A. Supplementary data

Supplementary data to this article can be found online at https://doi.org/10.1016/j.nano.2019.102095.

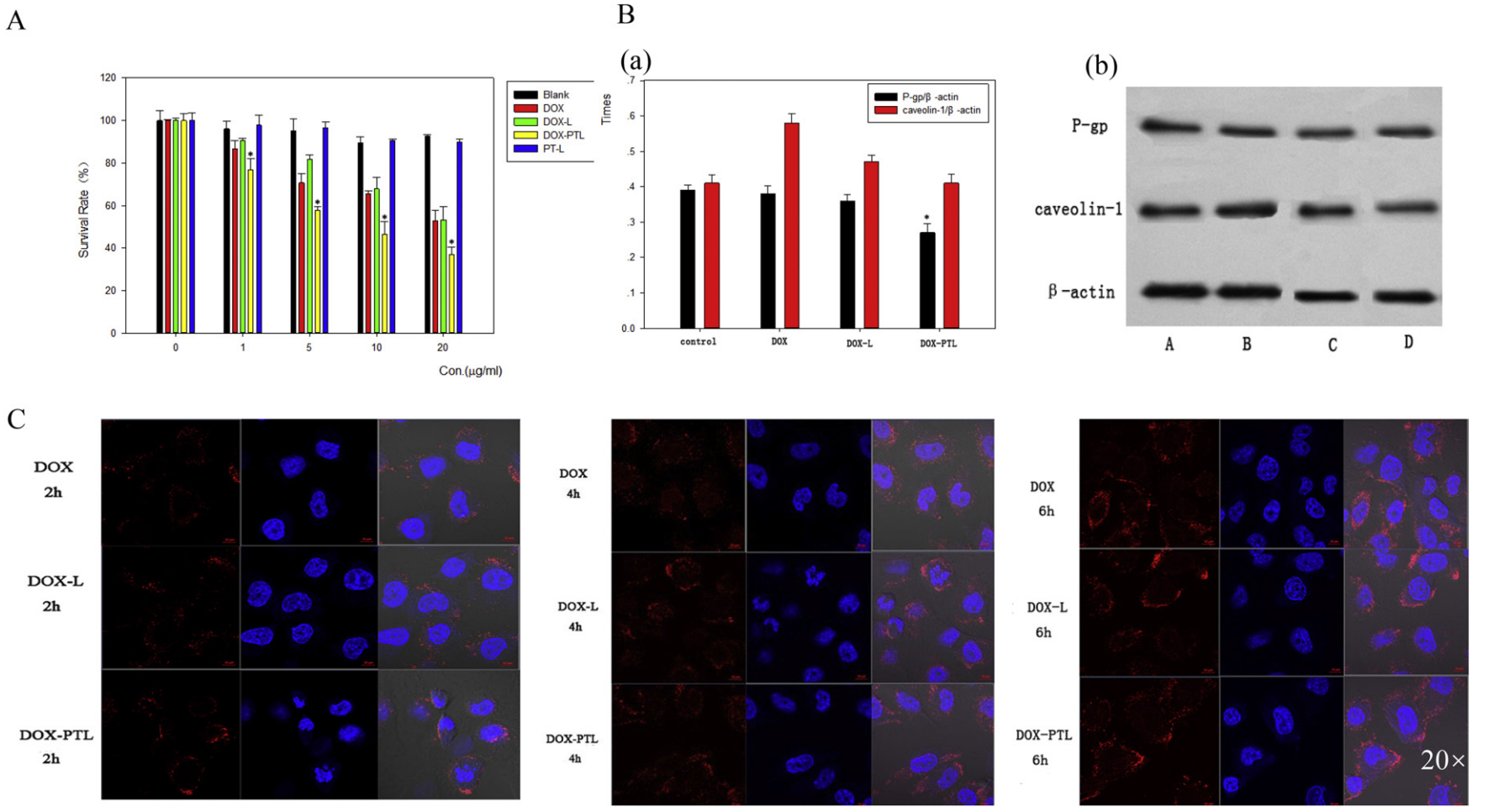

Figure 7. (**A**) MCF/ADR cytotoxicity associated with blank liposomes, free DOX, PT-L, DOX-L and DOX-PTL (n = 4). (**B, C**) The gray analysis and P-gp and caveolin-1 levels after treatment with a DOX solution, DOX-L and DOX-PTL. (**D**) Uptake of DOX, DOX-TL and DOX-PTL by MCF/ADR cells. 20×.

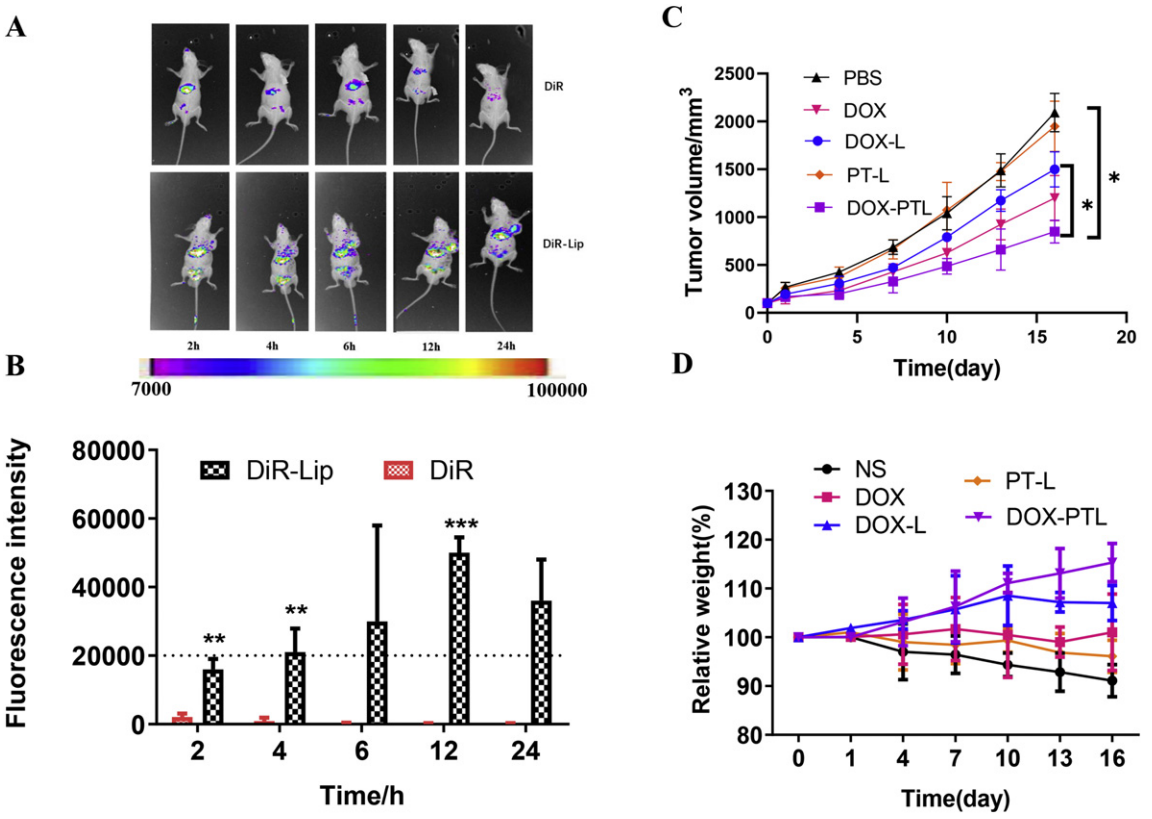

Figure 8. (**A, B**) *In vivo* imaging and quantitative analysis of tumor-bearing mice after the administration of DiR and DiR-L (**$P < 0.01$, *** $P < 0.001$, *vs.* DiR group at the same time point). (**C**) The tumor growth curves after different treatment including saline, DOX, PT-L, DOX-L, PT-L and DOX-PTL (*$P < 0.05$, from two-way ANOVA, * $P < 0.05$, from *t* tests between groups). (**D**) Body weight changes for different group during treatment. Data are presented as mean ± SD ($n = 5$). * $P < 0.05$, ** $P < 0.01$, *** $P < 0.001$.

References

1. S. Dawar, N. Singh, R. K. Kanwar, R. L. Kennedy, R. N. Veedu, S. F. Zhou, et al. J. R. Kanwar, Multifunctional and multitargeted nanoparticles for drug delivery to overcome barriers of drug resistance in human cancers, *Drug discovery today*, 18(2013), pp., 1292–1300.
2. H. M. Coley, Mechanisms and strategies to overcome chemotherapy resistance in metastatic breast cancer, *Cancer treatment reviews*, 34 (2008), pp., 378–390.
3. G. Szakacs, M. D. Hall, M. M. Gottesman, A. Boumendjel, R. Kachadourian, B. J. Day, et al. A. Di Pietro, Targeting the Achilles heel of multidrug-resistant cancer by exploiting the fitness cost of resistance, *Chemical reviews*, 114(2014), pp., 5753–5774.
4. J. L. Markman, A. Rekechenetskiy, E. Holler and J. Y. Ljubimova, Nanomedicine therapeutic approaches to overcome cancer drug resistance, *Adv Drug Deliv Rev*, 65(2013), pp., 1866–1879.
5. A. K. Iyer, A. Singh, S. Ganta and M. M. Amiji, Role of integrated cancer nanomedicine in overcoming drug resistance, *Adv Drug Deliv Rev*, 65(2013), pp., 1784–1802.
6. G. Szakacs, J. K. Paterson, J. A. Ludwig, C. Booth-Genthe and M. M. Gottesman, Targeting multidrug resistance in cancer, *Nature reviews. Drug discovery*, 5(2006), pp., 219–234.
7. G. Batist, K. A. Gelmon, K. N. Chi, W. H. Miller, Jr., S. K. Chia, L. D. Mayer, et al. A. C. Louie, Safety, pharmacokinetics, and efficacy of CPX-1 liposome injection in patients with advanced solid tumors, *Clin Cancer Res*, 15(2009), pp., 692–700.
8. Y. Chen, W. Zhang, Y. Huang, F. Gao, X. Sha and X. Fang, Pluronic-based functional polymeric mixed micelles for co-delivery of doxorubicin and paclitaxel to multidrug resistant tumor, *International journal of pharmaceutics*, 488(2015), pp., 44–58.
9. Y. Mi, J. Zhao and S. S. Feng, Targeted co-delivery of docetaxel, cisplatin and herceptin by vitamin E TPGS-cisplatin prodrug nanoparticles for multimodality treatment of cancer, *J Control Release*, 169 (2013), pp., 185–192.
10. J. Duan, H. M. Mansour, Y. Zhang, X. Deng, Y. Chen, J. Wang, et al. J. Zhao, Reversion of multidrug resistance by co-encapsulation of doxorubicin and curcumin in chitosan/poly(butyl cyanoacrylate) nanoparticles, *International journal of pharmaceutics*, 426(2012), pp., 193–201.
11. D. Pramanik, N. R. Campbell, S. Das, S. Gupta, V. Chenna, S. Bisht, et al. A. Maitra, A composite polymer nanoparticle overcomes multidrug resistance and ameliorates doxorubicin-associated cardiomyopathy, *Oncotarget*, 3(2012), pp., 640–650.
12. Z. Shi, S. Jain, I. W. Kim, X. X. Peng, I. Abraham, D. T. Youssef, et al. Z. S. Chen, Sipholenol A, a marine-derived sipholane triterpene, potently reverses P-glycoprotein (ABCB1)-mediated multidrug resistance in cancer cells, *Cancer science*, 98(2007), pp., 1373–1380.
13. S. Cheng, K. Swanson, I. Eliaz, J. N. McClintick, G. E. Sandusky and D. Sliva, Pachymic acid inhibits growth and induces apoptosis of pancreatic cancer in vitro and in vivo by targeting ER stress, *PloS one*, 10(2015), pp., e0122270.
14. J. H. Kim, S. R. Kim, I. S. Song, H. J. Shin, H. S. Kim, J. H. Lee, et al. Y. C. Shin, Different transport activity of human triallelic MDR1 893Ala/Ser/Thr variant and its association with herb extracts, *Phytotherapy research : PTR*, 25(2011), pp., 1141–1147.

15. G. Minotti, P. Menna, E. Salvatorelli, G. Cairo and L. Gianni, Anthracyclines: molecular advances and pharmacologic developments in antitumor activity and cardiotoxicity, *Pharmacological reviews*, 56 (2004), pp., 185–229.
16. M. Pajic, J. K. Iyer, A. Kersbergen, E. van der Burg, A. O. Nygren, J. Jonkers, et al. S. Rottenberg, Moderate increase in Mdr1a/1b expression causes in vivo resistance to doxorubicin in a mouse model for hereditary breast cancer, *Cancer research*, 69(2009), pp., 6396–6404.
17. T. Chen, Hua, G. Chou, X. Mao and X. Zou, A unique naphthone derivative and a rare 4,5-seco-lanostane triterpenoid from Poria cocos, *Molecules*, 23(2018), pp.
18. T. Tai, A. Akahori and T. Shingu, A Lanostane Triterpenoid from Poria-Cocos, *Phytochemistry*, 31(1992), pp., 2548–2549.
19. T. Tai, A. Akahori and T. Shingu, Triterpenes of Poria-Cocos, *Phytochemistry*, 32(1993), pp., 1239–1244.
20. G. Fiucci, D. Ravid, R. Reich and M. Liscovitch, Caveolin-1 inhibits anchorage-independent growth, anoikis and invasiveness in MCF-7 human breast cancer cells, *Oncogene*, 21(2002), pp., 2365–2375.
21. J. Fernandes, R. O. Castilho, M. R. da Costa, K. Wagner-Souza, M. A. Coelho Kaplan and C. R. Gattass, Pentacyclic triterpenes from Chrysobalanaceae species: cytotoxicity on multidrug resistant and sensitive leukemia cell lines, *Cancer Lett*, 190(2003), pp., 165–169.
22. D. R. Vogus, M. A. Evans, A. Pusuluri, A. Barajas, M. Zhang, V. Krishnan, et al. S. Mitragotri, A hyaluronic acid conjugate engineered to synergistically and sequentially deliver gemcitabine and doxorubicin to treat triple negative breast cancer, *J Control Release*, 267(2017), pp., 191–202.
23. Z. Zhao, S. Lou, Y. Hu, J. Zhu and C. Zhang, A nano-in-nano polymer-dendrimer nanoparticle-based nanosystem for controlled multidrug delivery, *Molecular pharmaceutics*, 14(2017), pp., 2697–2710.
24. S. Lou, Z. Zhao, M. Dezort, T. Lohneis and C. Zhang, Multifunctional nanosystem for targeted and controlled delivery of multiple chemotherapeutic agents for the treatment of drug-resistant breast cancer, *ACS omega*, 3(2018), pp., 9210–9219.
25. J. Yu, H. Chen, L. Jiang, J. Wang, J. Dai and J. Wang, Codelivery of adriamycin and P-gp inhibitor quercetin using PEGylated liposomes to overcome cancer drug resistance, *Journal of pharmaceutical sciences*, 108(2019), pp., 1788–1799.